nature nanotechnology

LETTERS

PUBLISHED ONLINE: 23 FEBRUARY 2014 | DOI: 10.1038/NNANO.2014.13

Biosynthesis of magnetic nanostructures in a foreign organism by transfer of bacterial magnetosome gene clusters

Isabel Kolinko[1], Anna Lohße[1], Sarah Borg[1], Oliver Raschdorf[1,2], Christian Jogler[1†], Qiang Tu[3,4], Mihály Pósfai[5], Éva Tompa[5], Jürgen M. Plitzko[2,6], Andreas Brachmann[1], Gerhard Wanner[1], Rolf Müller[3], Youming Zhang[4]* and Dirk Schüler[1]*

The synthetic production of monodisperse single magnetic domain nanoparticles at ambient temperature is challenging[1,2]. In nature, magnetosomes—membrane-bound magnetic nanocrystals with unprecedented magnetic properties—can be biomineralized by magnetotactic bacteria[3]. However, these microbes are difficult to handle. Expression of the underlying biosynthetic pathway from these fastidious microorganisms within other organisms could therefore greatly expand their nanotechnological and biomedical applications[4,5]. So far, this has been hindered by the structural and genetic complexity of the magnetosome organelle and insufficient knowledge of the biosynthetic functions involved. Here, we show that the ability to biomineralize highly ordered magnetic nanostructures can be transferred to a foreign recipient. Expression of a minimal set of genes from the magnetotactic bacterium *Magnetospirillum gryphiswaldense* resulted in magnetosome biosynthesis within the photosynthetic model organism *Rhodospirillum rubrum*. Our findings will enable the sustainable production of tailored magnetic nanostructures in biotechnologically relevant hosts and represent a step towards the endogenous magnetization of various organisms by synthetic biology.

The alphaproteobacterium *M. gryphiswaldense* produces uniform nanosized crystals of magnetite (Fe_3O_4), which can be engineered by genetic[6,7] and metabolic means[8] and are inherently biocompatible. The stepwise biogenesis of magnetosomes involves the invagination of vesicles from the cytoplasmic membrane, magnetosomal uptake of iron, and redox-controlled biomineralization of magnetite crystals, as well as their self-assembly into nanochains along a dedicated cytoskeletal structure to achieve one of the highest structural levels in a prokaryotic cell[3,9].

We recently discovered genes controlling magnetosome synthesis to be clustered within a larger (115 kb) genomic magnetosome island, in which they are interspersed by numerous genes of unrelated or unknown functions[6,10]. Although the smaller *mamGFDC*, *mms6* and *mamXY* operons have accessory roles in the biomineralization of properly sized and shaped crystals[6,11], only the large *mamAB* operon encodes factors essential for iron transport, magnetosome membrane (MM) biogenesis, and crystallization of magnetite particles, as well as their chain-like organization and intracellular positioning[6,10,12]. However, it has been unknown whether this gene set is sufficient for autonomous expression of magnetosome biosynthesis.

Using recombineering (recombinogenic engineering) based on phage-derived Red/ET homologous recombination, we stitched together several modular expression cassettes comprising all 29 genes (26 kb in total) of the four operons in various combinations (Supplementary Fig. 1), but lacking the tubulin-like *ftsZm*. This gene was omitted from its native *mamXY* operon because of its known interference with cell division during cloning. Regions 200–400 bp upstream of all operons were retained to ensure transcription from native promoters[13]. Transposable expression cassettes comprising the MycoMar (*tps*) or Tn5 transposase gene, two corresponding inverted repeats, the origin of transfer *oriT*, and an antibiotic resistance gene were utilized to enable transfer and random chromosomal integration in single copy[14,15] (Supplementary Tables 3 and 4). Chromosomal reintegration of all cassettes into different non-magnetic single-gene and operon deletion strains of *M. gryphiswaldense* resulted in stable wild type-like restoration of magnetosome biomineralization, indicating that transferred operons maintained functionality upon cloning and transfer (Supplementary Fig. 2).

We next attempted the transfer of expression cassettes to a foreign non-magnetic host organism (Fig. 1). We chose the photosynthetic alphaproteobacterium *R. rubrum* as a first model because of its biotechnological relevance and relatively close relationship to *M. gryphiswaldense*[16–18] (16S rRNA similarity to *M. gryphiwaldense* = 90%). Although the *mamAB* operon alone has been shown to support some rudimentary biomineralization in *M. gryphiswaldense*[6], neither genomic insertion of the *mamAB* operon alone (pTps_AB) nor in combination with the accessory *mamGFDC* genes (pTps_ABG) had any detectable phenotypic effect (Supplementary Table 1). We also failed to detect a magnetic response (C_{mag}) in the classical light scattering assay[19] after insertion of pTps_ABG6 (*mamAB* + *mamGFDC* + *mms6*). However, the cellular iron content of *R. rubrum_ABG6* increased 2.4-fold compared with the untransformed wild type (Supplementary Table 1). Transmission electron microscopy (TEM) revealed a loose chain

[1]Ludwig-Maximilians-Universität München, Department of Biology I, Großhaderner Straße 2-4, 82152 Martinsried, Germany, [2]Max Planck Institute of Biochemistry, Department of Molecular Structural Biology, Am Klopferspitz 18, 82152 Martinsried, Germany, [3]Helmholtz Institute for Pharmaceutical Research Saarland, Helmholtz Centre for Infection Research and Department of Pharmaceutical Biotechnology, Saarland University, PO Box 151150, 66041 Saarbrücken, Germany, [4]Shandong University – Helmholtz Joint Institute of Biotechnology, State Key Laboratory of Microbial Technology, Life Science College, Shandong University, Jinan 250100, China, [5]University of Pannonia, Department of Earth and Environmental Sciences, Veszprém, H-8200 Hungary, [6]Bijvoet Center for Biomolecular Research, Utrecht University, 3584 CH Utrecht, The Netherlands, [†]Present address: Leibniz Institute DSMZ, Department of Microbial Cell Biology and Genetics, Inhoffenstraße 7B, 38124 Braunschweig, Germany. *e-mail: dirk.schueler@lmu.de; zhangyouming@sdu.edu.cn

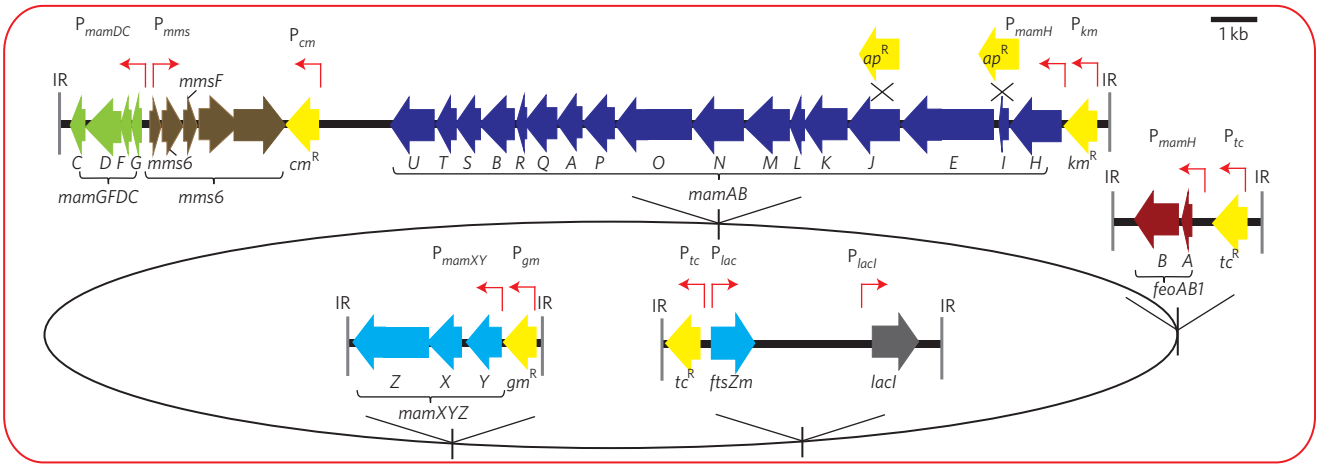

Figure 1 | Schematic representation of molecular organization of gene cassettes inserted into the chromosome of *R. rubrum* in a stepwise manner. Broad arrows indicate the extensions and transcriptional directions of individual genes. Different colours illustrate the cassettes inserted into the chromosome (oval shape, not to scale) as indicated by their gene names in the figure. Shown in yellow are antibiotic resistance genes (km^R, kanamycin resistance; tc^R, tetracycline resistance; ap^R, ampicillin resistance; gm^R, gentamicin resistance). Thin red arrows indicate different promoters (P) driving transcription of inserted genes (P_{km}, P_{gm}, P_{tc}, promoters of antibiotic resistance cassettes; P_{lacI}, promoter lac repressor; P_{mms}, P_{mamDC}, P_{mamH}, P_{mamXY}, native promoters of the respective gene clusters from *M. gryphiswaldense*; P_{lac}, *lac* promoter). Crossed lines indicate sites of gene deletions of *mamI* and *mamJ* in strains *R. rubrum_ABG6X_dI* and *R. rubrum_ABG6X_dJ*, respectively. IR, inverted repeat defining the boundaries of the sequence inserted by the transposase.

of small (~12 nm) irregularly shaped electron-dense particles (Fig. 2a,ii), identified as poorly crystalline hematite (Fe_2O_3) by analysis of the lattice spacings in high-resolution TEM images (Supplementary Fig. 3), much as in the hematite particles previously identified in *M. gryphiswaldense* mutants affected in crystal formation[11,20]. To further enhance biomineralization, we next transferred pTps_XYZ, an insertional plasmid harbouring *mamX*, *Y* and *Z* from the *mamXY* operon, into *R. rubrum_ABG6* (Supplementary Fig. 1). The resulting strain *ABG6X* encompassed all 29 relevant genes of the magnetosome island except *ftsZm*. Intriguingly, cells of *ABG6X* exhibited a significant magnetic response (Supplementary Table 1) and were 'magnetotactic', that is, within several hours accumulated as a visible pellet near a magnet at the edge of a culture flask (Fig. 2b). TEM micrographs revealed the presence of electron-dense particles identified as magnetite (Fe_3O_4) (Fig. 2d, Supplementary Fig. 8 and Table 1), which were aligned in short, fragmented chains loosely dispersed within the cell (Fig. 2a,iii). Despite their smaller sizes (average, 24 nm) the particles strongly resembled the magnetosomes of the donor strain in terms of their projected outlines and thickness contrast, suggestive of cubooctahedral or octahedral crystal morphologies (Fig. 2d). Additional insertion of the *ftsZm* gene under control of the inducible *lac* promoter had no effect on the cellular iron content and the number and size of magnetite crystals in the resulting *R. rubrum_ABG6X_ftsZm* (Fig. 2a,iv, Supplementary Table 1). Magnetite biomineralization occurred during microoxic chemotrophic as well anoxic photoheterotrophic cultivation. Medium light intensity, 50 μM iron and 23 °C supported the highest magnetic response (C_{mag}) and robust growth of the metabolically versatile *R. rubrum_ABG6X*, which was indistinguishable from the untransformed wild type (Supplementary Figs 4 and 5). The magnetic phenotype remained stable for at least 40 generations under non-selective conditions, with no obvious phenotypic changes.

To test whether known mutation phenotypes from *M. gryphiswaldense* could be replicated in *R. rubrum*, we constructed variants of expression cassettes in which single genes were omitted from the *mamAB* operon by deletion within the cloning host *Escherichia coli*. The small (77 amino acids) MamI protein was previously implicated in MM vesicle formation and found to be essential for magnetosome synthesis[12]. *R. rubrum_ABG6X-dI* failed to express magnetosome particles (Supplementary Fig. 10), which phenocopied a *mamI* deletion in the related *M. magneticum*[12]. Another tested example was MamJ, which is assumed to connect magnetosome particles to the cytoskeletal magnetosome filament formed by the actin-like MamK[21]. Much as in *M. gryphiswaldense*, deletion of *mamJ* caused agglomeration of magnetosome crystals in ~65% of *R. rubrum_ABG6X-dJ* cells (Fig. 2a,v, Supplementary Fig. 10 and Table 1). Together, these observations indicate that magnetosome biogenesis and assembly within the foreign host are governed by very similar mechanisms and structures as in the donor, which are conferred by the transferred genes.

As magnetosomes in *R. rubrum_ABG6X* were still smaller than those of *M. gryphiswaldense*, we wondered whether full expression of biomineralization may depend on the presence of further auxiliary functions, possibly encoded outside the canonical magnetosome operons. For instance, deletion of *feoB1* encoding a constituent of a ferrous iron transport system specific for magnetotactic bacteria caused fewer and smaller magnetosomes in *M. gryphiswaldense*[22]. Strikingly, insertion of *feoAB1* into *R. rubrum* strain *ABG6X* resulted in even larger, single-crystalline and twinned magnetosomes and longer chains (440 nm) (Fig. 2a,vi, Supplementary Table 1). The size (37 nm) of the crystals approached that of the donor, and cellular iron content was substantially increased (0.28% of dry weight) compared with *R. rubrum_ABG6X* (0.18%), although still lower than in *M. gryphiswaldense* (3.5%), partly because of the considerably larger volume of *R. rubrum* cells (Fig. 2c).

Magnetosome particles could be purified from disrupted cells by magnetic separation and centrifugation[23] and formed stable suspensions (Fig. 3). Isolated crystals were clearly enclosed by a layer of organic material resembling the MM attached to magnetosomes of *M. gryphiswaldense*. Smaller, immature crystals were surrounded by partially empty vesicles (Fig. 3c, inset), which were also seen in thin-sectioned cells (Supplementary Fig. 8) and on average were smaller (66 ± 6 nm) than the abundant photosynthetic intracytoplasmic membranes (ICMs) (93 ± 34 nm; Fig. 3a, Supplementary Fig. 8).

Organic material of the putative MM could be solubilized from isolated magnetite crystals of *R. rubrum_ABG6X* by various detergents (Fig. 3d), in a similar manner to that reported for MM of

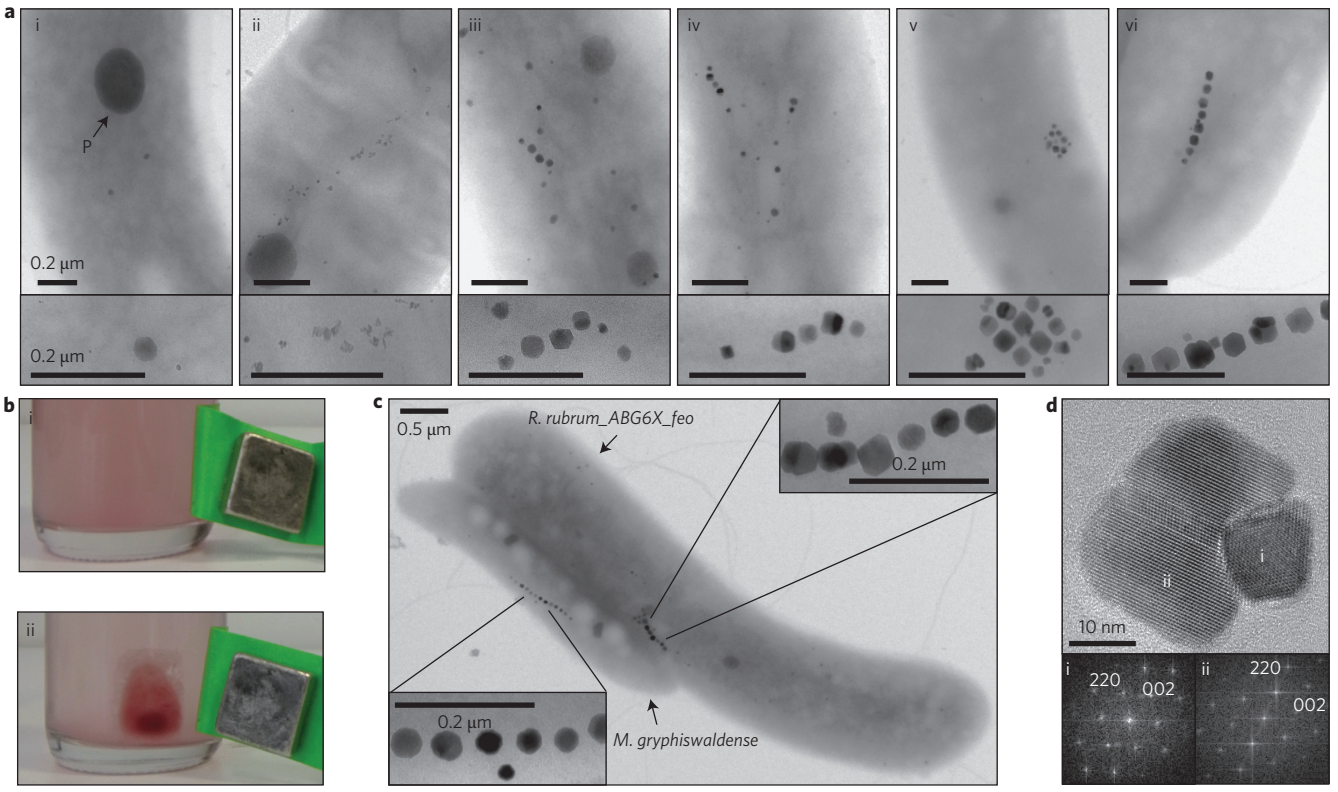

Figure 2 | Phenotypes of *R. rubrum* strains expressing different magnetosome gene clusters and auxiliary genes. a, TEM images: *R. rubrum* wild type (i), containing a larger phosphate inclusion (P) and some small, non-crystalline, electron-dense particles; *R. rubrum_ABG6* (ii); *R. rubrum_ABG6X* (iii); *R. rubrum_ABG6X_ftsZm* (iv); *R. rubrum_ABG6X_dJ* (v); *R. rubrum_ABG6X_feo* (vi). Insets: Magnifications of non-crystalline electron-dense particles (i) or heterologously expressed nanocrystals (ii–vi). All insets are of the same particles/crystals as in their respective main images, except for (v). For further TEM micrographs see Supplementary Fig. 10. **b**, Unlike the untransformed *R. rubrum* wild type, cells of *R. rubrum_ABG6X* accumulated as a visible red spot near the pole of a permanent magnet at the edge of a culture flask. **c**, TEM micrograph of a mixed culture of the donor *M. gryphiswaldense* and the recipient *R. rubrum_ABG6X_feo*, illustrating characteristic cell properties and magnetosome organization. Insets: Magnifications of magnetosomes from *M. gryphiswaldense* and *R. rubrum_ABG6X_feo*. **d**, High-resolution TEM lattice image of a twinned crystal from *R. rubrum_ABG6X*, with Fourier transforms (i) and (ii) showing intensity maxima consistent with the structure of magnetite.

M. gryphiswaldense[23]. Proteomic analysis of the SDS-solubilized MM revealed a complex composition (Supplementary Fig. 6), and several genuine magnetosome proteins (MamKCJAFDMBYOE, Mms6, MmsF) were detected among the most abundant polypeptides (Supplementary Table 2). An antibody against MamC, the most abundant protein in the MM of *M. gryphiswaldense*[23], also recognized a prominent band with the expected mass (12.4 kDa) in the MM of *R. rubrum_ABG6X* (Supplementary Fig. 6).

The subcellular localization of selected magnetosome proteins in *R. rubrum* depended on the presence of further determinants encoded by the transferred genes. For example, MamC tagged with a green fluorescent protein, which is commonly used as magnetosome chain marker in *M. gryphiswaldense*[24] displayed a punctuate pattern in the *R. rubrum* wild type background. In contrast, a filamentous fluorescent signal became apparent in the majority of cells (79%) of the *R. rubrum_ABG6X* background, in which the full complement of magnetosome genes is present (Supplementary Fig. 7), reminiscent of the magnetosome-chain localization of these proteins in *M. gryphiswaldense*[24].

Our findings demonstrate that one of the most complex prokaryotic structures can be functionally reconstituted within a foreign, hitherto non-magnetic host by balanced expression of a multitude of structural and catalytic membrane-associated factors. This also provides the first experimental evidence that the magnetotactic trait can be disseminated to different species by only a single event, or a few events, of transfer, which are likely to occur also under natural conditions by horizontal gene transfer as speculated before[18,25,26].

The precise functions of many of the transferred genes have remained elusive in native magnetotactic bacteria, but our results will now enable the dissection and engineering of the entire pathway in genetically more amenable hosts. The approximately 30 transferred magnetosome genes constitute an autonomous expression unit that is sufficient to transplant controlled synthesis of magnetite nanocrystals and their self-assembly within a foreign organism. However, further auxiliary functions encoded outside the *mam* and *mms* operons are necessary for biomineralization of donor-like magnetosomes. Nevertheless, this minimal gene set is likely to shrink further as a result of systematic reduction approaches in different hosts.

Importantly, the results are promising for the sustainable production of magnetic nanoparticles in biotechnologically relevant photosynthetic hosts. Previous attempts to magnetize both prokaryotic and eukaryotic cells by genetic and metabolic means (for example, refs 27,28) resulted in only irregular and poorly crystalline iron deposits. This prompted ideas to borrow genetic parts of the bacterial magnetosome pathway for the synthesis of magnetic nanoparticles within cells of other organisms[4,29]. Our results now set the stage for synthetic biology approaches to genetically endow both uni- and multicellular organisms with magnetization by biomineralization of tailored magnetic nanostructures. This might be exploited for instance in nanomagnetic actuators or *in situ* heat

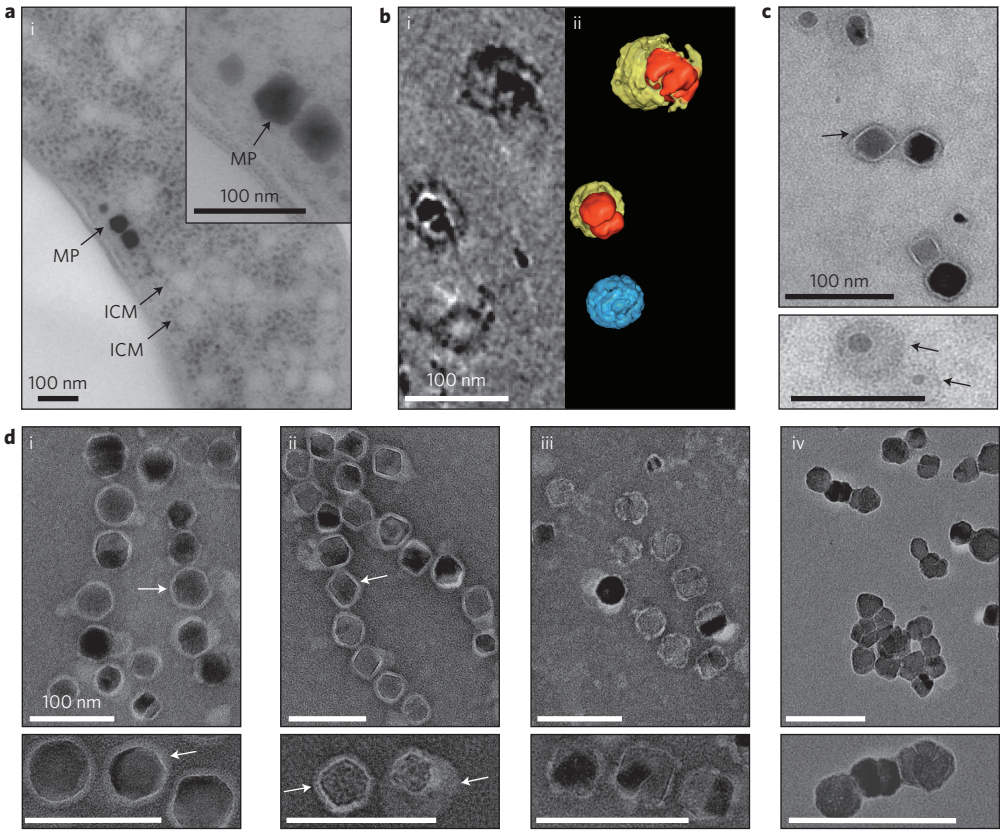

Figure 3 | Ultrastructural analysis of *R. rubrum_ABG6X* and isolated crystals. a, Cryo-fixed, thin-sectioned *R. rubrum_ABG6X* contained intracytoplasmic membranes (ICMs) (93±34 nm, $n=95$) and magnetic particles (MP). Inset: Magnification of the magnetite crystals. **b**, Cryo-electron tomography of isolated magnetic particles of *R. rubrum_ABG6X*: *x*–*y* slice of a reconstructed tomogram (i) and surface-rendered three-dimensional representation (ii). A membrane-like structure (yellow, thickness 3.4±1.0 nm, $n=6$) surrounds the magnetic particles (red). (Blue, empty vesicle.) **c**,**d**, TEM images of isolated magnetosomes from *R. rubrum_ABG6X* (**c** and **d**,ii, iii, iv) and *M. gryphiswaldense* (**d**,i) negatively stained by uranyl acetate (**c**) or phosphotungstic acid (**d**). Insets: Higher-magnification images of magnetic particles; these are of different particles to those shown in the main images, except for (iv). Scale bars, 100 nm. Arrows indicate the magnetosome membrane, which encloses magnetic crystals of *M. gryphiswaldense* (thickness 3.2±1.0 nm, $n=103$) and *R. rubrum_ABG6X* (thickness 3.6±1.2 nm, $n=100$). Organic material could be solubilized from magnetite crystals of *R. rubrum_ABG6X* with SDS (sodium dodecyl sulfate, iv) and less effectively also with Triton X-100 (iii).

generators in the emerging field of magnetogenetics[30], or for endogenous expression of magnetic reporters for bioimaging[31].

Methods

Bacterial strains, media and cultivation. The bacterial strains are described in Supplementary Table 4. *E. coli* strains were cultivated as previously described[32]. A volume of 1 mM DL-α,ε-diaminopimelic acid was added for the growth of auxotrophic strains BW29427 and WM3064. *M. gryphiswaldense* strains were cultivated in flask standard medium (FSM), in liquid or on plates solidified by 1.5% agar, and incubated at 30 °C under microoxic (1% O_2) conditions[33]. Cultures of *R. rubrum* strains were grown as specified (Supplementary Fig. 3).

Construction of magnetosome gene cluster plasmids and conjugative transfer. The oligonucleotides and plasmids used in this study are listed in Supplementary Tables 4 and 5. Red/ET (Lambda red and RecET) recombination was performed as described previously[14]. Briefly, a cloning cassette was amplified by polymerase chain reaction (PCR) and transferred into electrocompetent *E. coli* cells (DH10b) expressing phage-derived recombinases from a circular plasmid (pSC101-BAD-gbaA). After transfer of the cassette, recombination occurred between homologous regions on the linear fragment and the plasmid.

To stitch the magnetosome gene clusters together into a transposon plasmid (Supplementary Fig. 1) we used triple recombination[14] and co-transformed two linear fragments, which recombined with a circular plasmid. Recombinants harbouring the correct plasmids were selected by restriction analysis[32].

Conjugations into *M. gryphiswaldense* were performed as described before[33]. For conjugation of *R. rubrum*, cultures were incubated in ATCC medium 112. Approximately 2×10^9 cells were mixed with 1×10^9 *E. coli* cells, spotted on American Type Culture Collection (ATCC) 112 agar medium and incubated for 15 h. Cells were flushed from the plates and incubated on ATCC 112 agar medium supplemented with appropriate antibiotics for 7–10 days (Tc = 10 μg ml^{-1}; Km = 20 μg ml^{-1}; Gm = 10 μg ml^{-1}, where Tc, tetracycline; Km, kanamycin; Gm, gentamicin). Sequential transfer of the plasmids resulted in 1×10^{-6} to 1×10^{-8} antibiotic-resistant insertants per recipient, respectively. Two clones from each conjugation experiments were chosen for further analyses. Characterized insertants were indistinguishable from wild type with respect to motility, cell morphology or growth (Supplementary Fig. 5).

Analytical methods. The optical density of *M. gryphiswaldense* cultures was measured turbidimetrically at 565 nm as described previously[19]. The optical density of *R. rubrum* cultures was measured at 660 nm and 880 nm. The ratio of 880/660 nm was used to determine yields of chromatophores within intact cells (Supplementary Fig. 4). Furthermore, *bacteriochlorophyll a* was extracted from cultures with methanol. Absorption spectra (measured in an Ultrospec 3000 photometer, GE Healthcare) of photoheterotrophically cultivated *R. rubrum_ABG6X* cells were indistinguishable from that of the wild type (Supplementary Fig. 4). The average magnetic orientation of cell suspensions (C_{mag}) was assayed with a light scattering assay as described previously[19]. Briefly, cells were aligned at different angles to a light beam by application of an external magnetic field.

Microscopy. For TEM of whole cells and isolated magnetosomes, specimens were directly deposited onto carbon-coated copper grids. Magnetosomes were stained with 1% phosphotungstic acid or 2% uranyl acetate. Samples were viewed and recorded with a Morgagni 268 microscope. Sizes of crystals and vesicles were measured with ImageJ software.

Chemical fixation, high-pressure freezing and thin sectioning of cells were performed as described previously[17]. Processed samples were viewed with an EM 912 electron microscope (Zeiss) equipped with an integrated OMEGA energy filter operated at 80 kV in the zero loss mode. Vesicle sizes were measured with ImageJ software. High-resolution TEM was performed with a JEOL 3010 microscope,

operated at 297 kV and equipped with a Gatan Imaging Filter for the acquisition of energy-filtered compositional maps. For TEM data processing and interpretation, DigitalMicrograph and SingleCrystal software were used[20]. Cryo-electron tomography was performed as described previously[21]. Fluorescence microscopy was performed with an Olympus IX81 microscope equipped with a Hamamatsu Orca AG camera using exposure times of 0.12–0.25 s. Image rescaling and cropping were performed with Photoshop 9.0 software.

Received 9 September 2013; accepted 16 January 2014; published online 23 February 2014

References

1. Prozorov, T., Bazylinski, D. A., Mallapragada, S. K. & Prozorov, R. Novel magnetic nanomaterials inspired by magnetotactic bacteria: topical review. *Mater. Sci. Eng. R* **74,** 133–172 (2013).
2. Baumgartner, J., Bertinetti, L., Widdrat, M., Hirt, A. M. & Faivre, D. Formation of magnetite nanoparticles at low temperature: from superparamagnetic to stable single domain particles. *PLoS ONE* **8,** e57070 (2013).
3. Bazylinski, D. A. & Frankel, R. B. Magnetosome formation in prokaryotes. *Nature Rev. Microbiol.* **2,** 217–230 (2004).
4. Goldhawk, D. E., Rohani, R., Sengupta, A., Gelman, N. & Prato, F. S. Using the magnetosome to model effective gene-based contrast for magnetic resonance imaging. *Wiley Interdiscip. Rev. Nanomed. Nanobiotechnol.* **4,** 378–388 (2012).
5. Murat, D. Magnetosomes: how do they stay in shape? *J. Mol. Microbiol. Biotechnol.* **23,** 81–94 (2013).
6. Lohsse, A. *et al.* Functional analysis of the magnetosome island in *Magnetospirillum gryphiswaldense*: the *mamAB* operon is sufficient for magnetite biomineralization. *PLoS ONE* **6,** e25561 (2011).
7. Pollithy, A. *et al.* Magnetosome expression of functional camelid antibody fragments (nanobodies) in *Magnetospirillum gryphiswaldense*. *Appl. Environ. Microbiol.* **77,** 6165–6171 (2011).
8. Staniland, S. *et al.* Controlled cobalt doping of magnetosomes *in vivo*. *Nature Nanotech.* **3,** 158–162 (2008).
9. Jogler, C. & Schüler, D. Genomics, genetics, and cell biology of magnetosome formation. *Annu. Rev. Microbiol.* **63,** 501–521 (2009).
10. Ullrich, S., Kube, M., Schübbe, S., Reinhardt, R. & Schüler, D. A hypervariable 130-kilobase genomic region of *Magnetospirillum gryphiswaldense* comprises a magnetosome island which undergoes frequent rearrangements during stationary growth. *J. Bacteriol.* **187,** 7176–7184 (2005).
11. Raschdorf, O., Müller, F. D., Pósfai, M., Plitzko, J. M. & Schüler, D. The magnetosome proteins MamX, MamZ and MamH are involved in redox control of magnetite biomineralization in *Magnetospirillum gryphiswaldense*. *Mol. Microbiol.* **89,** 872–886 (2013).
12. Murat, D., Quinlan, A., Vali, H. & Komeili, A. Comprehensive genetic dissection of the magnetosome gene island reveals the step-wise assembly of a prokaryotic organelle. *Proc. Natl Acad. Sci. USA* **107,** 5593–5598 (2010).
13. Schübbe, S. *et al.* Transcriptional organization and regulation of magnetosome operons in *Magnetospirillum gryphiswaldense*. *Appl. Environ. Microbiol.* **72,** 5757–5765 (2006).
14. Fu, J. *et al.* Efficient transfer of two large secondary metabolite pathway gene clusters into heterologous hosts by transposition. *Nucleic Acids Res.* **36,** e113 (2008).
15. Martinez-Garcia, E., Calles, B., Arevalo-Rodriguez, M. & de Lorenzo, V. pBAM1: an all-synthetic genetic tool for analysis and construction of complex bacterial phenotypes. *BMC Microbiol.* **11,** 38 (2011).
16. Richter, M. *et al.* Comparative genome analysis of four magnetotactic bacteria reveals a complex set of group-specific genes implicated in magnetosome biomineralization and function. *J. Bacteriol.* **189,** 4899–4910 (2007).
17. Jogler, C. *et al.* Conservation of proteobacterial magnetosome genes and structures in an uncultivated member of the deep-branching *Nitrospira phylum*. *Proc. Natl Acad. Sci. USA* **108,** 1134–1139 (2011).
18. Lefèvre, C. T. *et al.* Monophyletic origin of magnetotaxis and the first magnetosomes. *Environ. Microbiol.* **15,** 2267–2274 (2013).
19. Schüler, D. R., Uhl, R. & Bäuerlein, E. A simple light scattering method to assay magnetism in *Magnetospirillum gryphiswaldense*. *FEMS Microbiol. Ecol.* **132,** 139–145 (1995).
20. Uebe, R. *et al.* The cation diffusion facilitator proteins MamB and MamM of *Magnetospirillum gryphiswaldense* have distinct and complex functions, and are involved in magnetite biomineralization and magnetosome membrane assembly. *Mol. Microbiol.* **82,** 818–835 (2011).
21. Scheffel, A. *et al.* An acidic protein aligns magnetosomes along a filamentous structure in magnetotactic bacteria. *Nature* **440,** 110–114 (2006).
22. Rong, C. *et al.* Ferrous iron transport protein B gene (feoB1) plays an accessory role in magnetosome formation in *Magnetospirillum gryphiswaldense* strain MSR-1. *Res. Microbiol.* **159,** 530–536 (2008).
23. Grünberg, K. *et al.* Biochemical and proteomic analysis of the magnetosome membrane in *Magnetospirillum gryphiswaldense*. *Appl. Environ. Microbiol.* **70,** 1040–1050 (2004).
24. Lang, C. & Schüler, D. Expression of green fluorescent protein fused to magnetosome proteins in microaerophilic magnetotactic bacteria. *Appl. Environ. Microbiol.* **74,** 4944–4953 (2008).
25. Jogler, C. *et al.* Comparative analysis of magnetosome gene clusters in magnetotactic bacteria provides further evidence for horizontal gene transfer. *Environ. Microbiol.* **11,** 1267–1277 (2009).
26. Jogler, C. *et al.* Toward cloning of the magnetotactic metagenome: identification of magnetosome island gene clusters in uncultivated magnetotactic bacteria from different aquatic sediments. *Appl. Environ. Microbiol.* **75,** 3972–3979 (2009).
27. Nishida, K. & Silver, P. A. Induction of biogenic magnetization and redox control by a component of the target of rapamycin complex 1 signaling pathway. *PLoS Biol.* **10,** e1001269 (2012).
28. Kim, T., Moore, D. & Fussenegger, M. Genetically programmed superparamagnetic behavior of mammalian cells. *J. Biotechnol.* **162,** 237–245 (2012).
29. Murat, D. *et al.* The magnetosome membrane protein, MmsF, is a major regulator of magnetite biomineralization in *Magnetospirillum magneticum* AMB-1. *Mol. Microbiol.* **85,** 684–699 (2012).
30. Huang, H., Delikanli, S., Zeng, H., Ferkey, D. M. & Pralle, A. Remote control of ion channels and neurons through magnetic-field heating of nanoparticles. *Nature Nanotech.* **5,** 602–606 (2010).
31. Westmeyer, G. G. & Jasanoff, A. Genetically controlled MRI contrast mechanisms and their prospects in systems neuroscience research. *Magn. Reson. Imaging* **25,** 1004–1010 (2007).
32. Sambrook, J. & Russell, D. *Molecular Cloning: A Laboratory Manual* Vol. 3 (Cold Spring Harbor Laboratory Press, 2001).
33. Kolinko, I., Jogler, C., Katzmann, E. & Schüler, D. Frequent mutations within the genomic magnetosome island of *Magnetospirillum gryphiswaldense* are mediated by RecA. *J. Bacteriol.* **193,** 5328–5334 (2011).

Acknowledgements

This work was supported by the Human Frontier Science Foundation (grant RGP0052/2012), the Deutsche Forschungsgemeinschaft (grants SCHU 1080/12-1 and 15-1) and the European Union (Bio2MaN4MRI). The authors thank F. Kiemer for expert help with iron measurements and cultivation experiments.

Author contributions

I.K., D.S., Y.Z., Q.T., C.J. and R.M. planned and performed cloning experiments. I.K. and A.L. performed genetic transfers and cultivation experiments. G.W. prepared cryo- and chemically fixed cells. S.B., O.R. and G.W. performed TEM and I.K. analysed the data. J.P. and O.R. performed cryo-electron tomography experiments. E.T. and M.P. took high-resolution TEM micrographs and analysed the data. I.K. and A.L. took fluorescence micrographs and performed phenotypization experiments. I.K. performed western blot experiments and analysed proteomic data. A.B. performed Illumina genome sequencing and I.K. analysed the data. I.K. and D.S. designed the study and wrote the paper. All authors discussed the results and commented on the manuscript.

Additional information

Supplementary information is available in the online version of the paper. Reprints and permissions information is available online at www.nature.com/reprints. Correspondence and requests for materials should be addressed to Y.Z. and D.S.

Competing financial interests

I.K. and D.S. (LMU Munich) have filed a patent application on the process described in this work (Production of magnetic nanoparticles in recombinant host cells, EP13193478).

NANOPARTICLE BIOSYNTHESIS

An accommodating host

A commercially viable method for synthesizing magnetic nanoparticles could be developed by transferring clusters of genes from magnetic bacteria to foreign, more stable bacteria.

Sarah Staniland

Magnetic bacteria are a curious natural phenomenon. They are aquatic motile bacteria that take up iron from the surrounding solution and use it to make an internal chain of nanomagnetic particles within lipid vesicles (known as magnetosome chains). As a result, the bacteria can align and swim along magnetic field lines[1]. The morphology of these nanoparticles varies between strains of bacteria, but is strictly controlled within each strain — different biomineralization proteins give rise to very narrow magnetosome size and shape distributions. These simple cells, therefore, have an incredible ability to synthesize nanomagnets with different nanoscale morphologies with biological precision[1]. Furthermore, the composition of the nanoparticles can be adjusted *in vivo* to tune their magnetic properties[2], and because the nanoparticles are produced within a lipid membrane they are inherently biocompatible. Extensive work in the field[3–6] has shown that the bacteria are able to produce the magnetosome vesicles, transport iron ions, and control the nucleation and crystallization of the magnetite nanoparticles by using a suite of proteins. These proteins are encoded in the genes on a section of the bacterial genome that is known as the 'magnetosome island'.

The bacteria are found in seas, rivers and ponds all over the world, and given how common they are, they could potentially be used to develop a practical method for producing nanomagnets. They are, however, extremely slow and difficult to culture outside their natural environment. One way to address this problem is to transfer the nanomagnet-making machinery into faster and easier growing bacteria, and researchers have been exploring the idea of transferring the magnetosome island, and thus the code for the biosynthesis of magnetosomes, into a less fastidious bacterium for a number of years. However, although the gene clusters within the magnetosome island that are required for biomineralization have been identified[3], successfully transferring these specific gene clusters or indeed the whole island to a different bacterium has remained an elusive goal. Writing in *Nature Nanotechnology,* Dirk Schüler, Youming Zhang and colleagues show that gene clusters from the magnetosome island of a strain of magnetic bacteria called *Magnetospirillum gryphiswaldense* can be transferred into the photosynthetic bacterium *Rhodospirillum rubrum*, and that the biosynthesis of magnetosomes can be instigated within these host cells[7] (Fig. 1).

The researchers — who are based at the Ludwig Maximilian University of Munich, the University of Pannonia, the Max Planck Institute of Biochemistry, Utrecht University, Saarland University and Shangdong University — successfully produced several expression cassettes, that is, pieces of DNA containing the target genes with the ability to produce the proteins necessary for magnetosome biosynthesis within a different bacterium. These cassettes contain the four main gene clusters on the magnetosome island that have previously been shown to be either essential (*mamAB*) or regulatory (*mamGFDC*, *mms6* and *mamXY*) in magnetosome formation. The expression cassettes were transferred into *R. rubrum* and grown under the same conditions (iron ions in solution, microaerobic or anaerobic environment) as *M. gryphiswaldense* to see if magnetosomes could form. The host cells were found to be able to produce iron oxide particles of varying quality depending on which gene clusters were transferred. When the three gene clusters *mamAB*, *mamGFDC* and *mms6* were inserted into *R. rubrum*, the host produced very small, irregular, non-magnetic iron oxide particles. When *mamXY* was added to this expression cassette, short chains of small magnetosome-like particles were produced. Notably, when an iron uptake gene cluster (*feoAB1*) was also added to this expression cassette and inserted into *R. rubrum,* chains

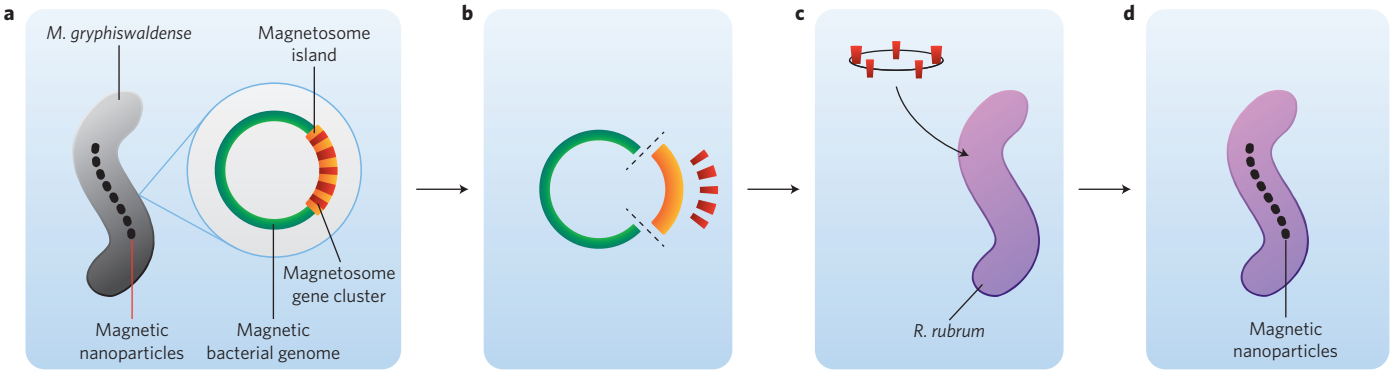

Figure 1 | Biosynthesis of magnetic nanoparticle chains in a foreign host. **a**, The genes controlling magnetosome production in *M. gryphiswaldense* exist within the genome, on the magnetosome island grouped into clusters. **b**–**d**, The essential gene clusters were extracted (**b**), cloned, recombined and inserted into the genome of the more robust bacterium, *R. rubrum* (**c**), resulting in the biosynthesis of magnetosomes (**d**).

of full-sized magnetosomes were formed, showing that the genes from the five clusters are all that is needed to biosynthesize magnetosomes in a new host.

R. rubrum is an obvious and logical choice of host for this experiment because it is the most similar model organism to *M. gryphiswaldense* (90% genetic similarity). Furthermore, *R. rubrum* is an interesting biotechnological organism, researched for its photosynthetic properties, as well as its ability to biodegrade plastics and produce hydrogen gas. Although the researchers have made an important advance in developing the production of nanomagnets in alternative hosts by using this bacterium, a crucial next step will be to instigate magnetosome biosynthesis in *Escherichia coli*, which is by far the most widely used model bacterium and, therefore, well characterized. Furthermore, the entire microbiological and biotechnology industries are based on this easy-to-grow microbe.

The synthesis of magnetosomes within another organism increases the possibility of commercialization of tailored magnetosome production within bacteria. If fast-growing microbes can be used in the future to produce uniform and physically tailored nanomagnets, a route to high-yield, greener and high-precision production methods for nanomagnets may emerge. Within a well-understood model organism, flexibility could be added to the production process such as tuning the magnetism with dopants[1] or genetic manipulation to enable the addition of functional molecules (such as drugs) to the lipid coating[8]. Furthermore, this technology may also allow the development of new magnetic tools in biotechnology. For example, vectors could be designed with a magnetosome expression cassette that could be interrupted when specific transformations occur, rendering them non-magnetic under these circumstances and magnetic otherwise, and therefore allowing them to be magnetically separated with ease. Similarly, this functionality could be used for magnetic separation to recover or concentrate valuable biotechnological cells in a range of industrial processes. ❐

Sarah Staniland is in the Department of Chemistry at the University of Sheffield, Dainton Building, Brook Hill, Sheffield S3 7HF, UK.
e-mail: s.s.staniland@sheffield.ac.uk

References
1. Bazylinski, D. A. & Frankel, R. B. *Nature Rev. Microbiol.* **2,** 217–230 (2004).
2. Staniland, S. *et al. Nature Nanotech.* **3,** 158–162 (2008).
3. Murat, D., Quinlan, A., Vali, H. & Komeili, A. *Proc. Natl Acad. Sci. USA* **107,** 5593–5598 (2010).
4. Ullrich, S., Kube, M., Schübbe, S., Reinhardt, R. & Schüler, D. *J. Bacteriol.* **187,** 7176–7184 (2005).
5. Richter, M. *et al. J. Bacteriol.* **189,** 4899–4910 (2007).
6. Tanaka, M. *et al. Proteomics* **19,** 5234–5247 (2006).
7. Kolinko, I. *et al. Nature Nanotech.* **9,** 193–197 (2014).
8. Kanetsuki, Y., Tanaka, M., Tanaka, T., Matsunaga, T. & Yoshino, T. *Biochem. Biophys. Res. Comm.* **426,** 7–11 (2012).

Published online: 23 February 2014

MECHANOCHEMISTRY

Molecules under pressure

Individual molecules change their conformation on application of an anisotropic compressive stress from the tip of an atomic force microscope.

Claus A. M. Seidel and Ralf Kühnemuth

Striving for the ultimate limit of control, researchers in nanotechnology are pushing the resolution of chemical transformations to the single-molecule, or even single-bond, level. Heat, light and electricity traditionally used to activate chemical bonds do not usually have the required spatial resolution and selectivity to exert such a fine control over chemical transformations. To this end, a mechanical stimulus has been proposed to manipulate atomic and molecular interactions[1,2]. In contrast to thermal energy, external forces provide mild reaction conditions by lowering the effective activation energy of a given chemical transformation (Fig. 1). Tensile stress, in particular, can change molecular conformations and induce bond scission, as well as, at a supramolecular level, cause molecular chain slippage, and folding and unfolding of proteins. To study transformations that involve no bond breaking, however, the amount of tensile stress that can be exerted is limited to the smaller conformational energies of the molecule. Now, writing in *Nature Nanotechnology*, Gerald Hinze, Thomas Basché and colleagues from the Johannes Gutenberg University of Mainz and the Max-Planck Institute for polymer research in Germany, report an experiment in which single-molecule mechanochemistry is carried out in compressive mode[3].

In their experiment, Hinze and colleagues used an atomic force microscope (AFM) tip to apply a localized compressive force on an isolated dye molecule on a mica surface. They selected a relatively large multichromophore fluorescent molecule with a diameter of about 2 nm so as to match the limited spatial resolution of their AFM tip. The dye is composed of four perylenediimide (PDI) units flexibly linked to a central terrylenediimide (TDI) core. The compressive stress applied by the AFM tip is redistributed throughout the conformational flexible structure of the molecule (Fig. 1). By measuring the fluorescence spectra of individual molecules as a function of the applied force, the researchers could monitor the effect of the compressive stress on the electronic states of the dye. In 47 out of 60 experiments, they observed a fluorescence emission shift to either shorter or longer wavelengths. In some cases, the shift was reversible when the tip was retracted, but in other cases the shift persisted for several seconds, thus proving that the electromagnetic interaction between the tip and the molecule was negligible. Using quantum-mechanical calculations, the German groups assigned the persistent spectral shifts to the emission from one of the five different possible conformers of TDI-4PDI that should be expected under equilibrium conditions.

Previous works on anisotropic mechanochemistry of fluorophores have also quantitatively investigated the effect of an applied force, F, to the electronic transition energy, E. In particular, it is instructive to compare relative parameters such as the force-induced spectral shift, $\Delta E/\Delta F$, obtained for tensile stress applied to penta-paraphenylenevinylene derivatives $(OPV)_5$ (ref. 4). In that work, the spectral shift was found to be linearly proportional to the external force, with an average slope $\Delta E/\Delta F$ of 0.03 eV nN^{-1}. Using quantum-mechanical calculations, the researchers